Geometric and Spectral Corrections to Multiple Solar Zenith Angle Satellite Data, Tasmania, Australia.

Mick Russell and Manuel Nunez

Department of Geography & Environmental Studies, University of Tasmania.

Abstract -- In order to examine the climatology of a number of low open vegetation types in Tasmania, the use of satellite derived instantaneous estimates of reflectance to monitor changes in the surface solar radiation exchange is examined. Field measurements of surface nadir narrow-band bi-directional reflectance (BR) and of broad-band hemispherical albedo (albedo) were carried out over a number of low vegetation types in Tasmania. The response of the measured surface reflectance to changes in illumination angle is used to develop a model to correct satellite images for solar zenith angle. A negative relationship is found to exist between narrow-field-of-view, narrow-band reflectance and albedo. From examination of off-nadir reflectance the negative relationship is found to be influenced by an increase in specular reflectance at high solar zenith angles and the incorporation of hot spot effects in nadir measurements at low solar zenith angles. A hysteresis about local noon solar zenith angles is found in the relationship of albedo with solar zenith angle. When normalised to a single solar zenith angle, reflectance is shown to exhibit a more consistent relationship with illumination angle than that of albedo. As a result it is proposed that the red and near infrared bands should be corrected to a common solar zenith angle before the application of narrow-band to broad-band and narrow-field-of-view to hemispherical corrections.

INTRODUCTION

The net input of solar radiation onto the earth's surface is controlled by the albedo, or solar hemispherical reflectance. Remote sensing offers methods of measuring albedo at high spatial or temporal resolution, Henderson-Sellers [1980]. Cloud cover amount can be determined by satellite and clear sky pixels can be used to estimate the input of solar radiation onto the surface for incorporation into net daily radiation models, Nunez and Kalma [1996].

In order to extract albedo from narrow-band narrow-field-of-view radiance measurements, both radiometric and geometric corrections must be applied, Qi *et al.* [1994]. Geometric corrections are required to account for both sun angle and canopy characteristics, Kimes and Sellers [1985]. As a result, it can be expected that different vegetation communities will exhibit varying changes in albedo throughout the passage of a day. However for each vegetation type it may be expected that geometric corrections will be required only for changes in solar zenith angle. This paper reviews temporal aspects of these corrections and shows that temporal correction must also be applied to changes in illumination angle.

Tasmania extends from the latitudes 40°S to 42°S. A number of low vegetation types are found throughout the island. A simplified map of the present range of each of the vegetation types used in this study is shown in Figure 1.

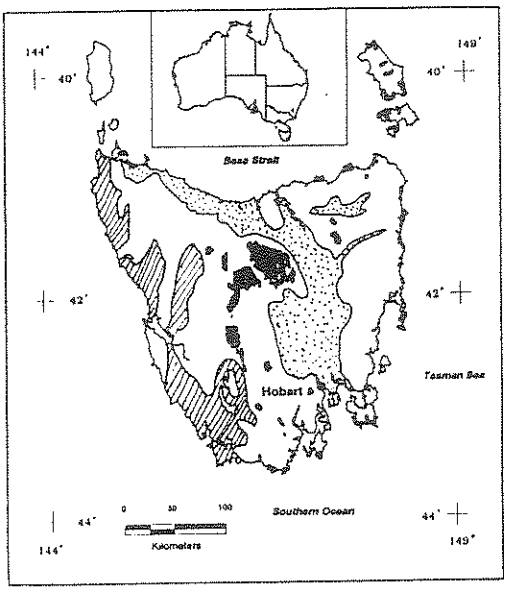

Figure 1. Location of Tasmania, showing the extent of wet heath (hatched), pasture (speckled), dry heath (black, on coastal areas) and alpine (black, inland), after Kirkpatrick and Dickinson [1974]

On the drier East coast, rainfall is 500 - 750 mm p.a., and a coastal heath community occurs within 1 to 2 km of the coast line. The west coast is exposed to zonal westerly winds resulting in high rainfall from 1500 - 9000 mm p.a. Nunez and Kirkpatrick [1996]. Due to the high rainfall on Western coastlines the allied community is wet-heath and is dominated by one graminoid, buttongrass, *Gymnoschoenus sphaerocephalus*, Jarman *et al.* [1988]. This community is found growing over peat from a few centimetres to 100 cm in depth and is locally known as buttongrass moorland after the dominant species. Anthropogenic burning over thousands of years has resulted in the extension of this vegetation type into large areas previously covered in temperate rainforest, Jackson [1981].

Both of the heath communities are made up almost exclusively of perennial evergreen shrubs and graminoids. The graminoids do not undergo senescence and rapid changes in biomass on an annual cycle do not occur. However short term drought, up to 2 months in length, may occur during summer of some years. Most components have scleromophic leaves and exhibit adaptations to fire, Kirkpatrick [1977].

Altitudes above 1000 m are vegetated with a complex alpine mosaic variously dominated by bolster shrubs, coniferous shrubs, other scleromorphic shrubs, tussock grasses and graminoids.

Central Tasmania has been extensively cleared for grazing and the resultant pasture vegetation is a mixture of predominantly exotic and native grasses.

In this study the results of measurements of surface albedo and narrowband reflectance that were carried out from 1995 to 1997 at a number of sites representative of each of the vegetation types is presented.

METHOD

Albedo was measured using two Kipp and Zonen pyranometers located on a 1.5 m arm mounted two metres above the canopy surface on a black painted aluminium stand. Reflected radiance was measured using a DELPHI radiometer with a 20° field of view mounted 2 m above the canopy. The instrument is fitted with filters that approximated the Landsat MSS channels.

Incoming narrowband irradiance was measured using an Island Research RADL-100 radiometer fitted with a plastic diffusing plate that gave a cosine response. This instrument, also fitted with filters that approximate the Landsat MSS, was calibrated against the DELPHI radiometer (also fitted with a cosine diffusing plate). Measured irradiance was divided by π to convert to incoming radiance.

When used to measure reflectance over the low vegetation types the narrowband instruments were mounted on a portable mount that could be moved along a 50 m transect. The DELPHI was mounted on a stationary wooden tripod when used to measure bidirectional reflectance (BR) distributions

An empirical model has been developed by Russell *et al.* [1997] to convert nadir measured reflectance in the AVHRR red and near-infrared bands to broadband hemispherical albedo. The model was based on data acquired at a solar zenith angle of 40°. As an extension of this model, a solar zenith angle of 40° was chosen as a basis for the normalisation of data acquired at other solar zenith angles.

RESULTS

Figure 2 shows the albedo measured over wet heath throughout the passage of one clear-sky day in summer. The other vegetation types studied exhibit similar shaped curves. The graph shows a relatively high albedo at high zenith angles and a minimum albedo at lower zenith angles around noon. Some hysteresis is evident about noon.

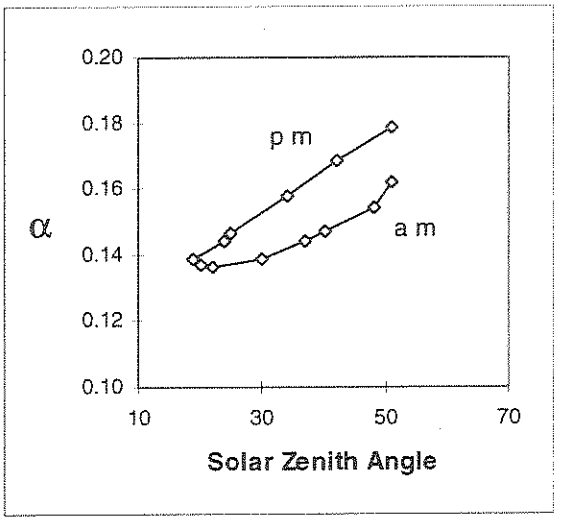

Figure 2. Albedo of wet heath community over the passage of a clear day in summer.

Figure 3 shows the progress of the nadir measured BR over two surface types. As the figure shows, in contrast to albedo, the nadir reflectance exhibits relatively low reflectance at high zenith angles and high reflectance around noon. This effect is more pronounced for the infrared channel and considerably more variation occurs for the dry-heath and alpine

vegetation due to the greater variation in cover evident in these vegetation types.

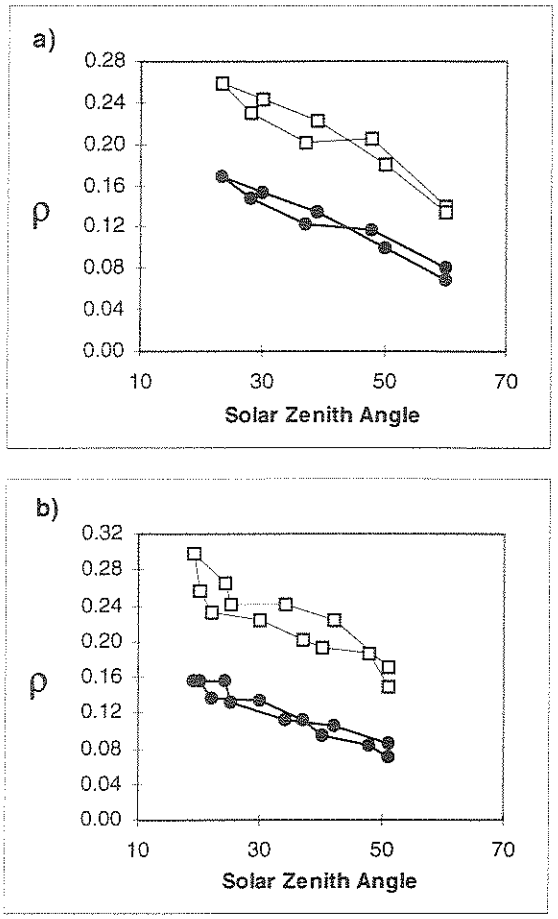

Figure 3. Nadir measured bidirectional reflectance over (a) wet heath and (b) dry heath in the red band (circles) and infrared band (squares), measured during summer.

Examining Figures 2 and 3, it appears that during the passage of one day, as albedo decreases, nadir reflectance increases and as albedo increases, nadir reflectance decreases. The reduced diurnal effects indicate that corrections for solar zenith angle would be more reliable for reflectance than for albedo.

For each of the vegetation types studied an average value of albedo or reflectance at a solar zenith angle of 40 was calculated. Each reflectance transect average or albedo measurement at all other zenith angles was compared to this standard value. The percentage deviation (D_n) from albedo or reflectance at Z = 40° was calculated using (1);

$$D_n = \frac{r_Z - r_{40}}{r_{40}} * 100 \qquad (1)$$

where r = reflectance or albedo at a solar zenith angle of 40° (40) or n (n).

Figure 4 shows the percentage albedo and reflectance difference graphed against zenith angle for all of the vegetation types studied. Despite the great variation in canopy characteristics the normalised reflectance shows a good relationship with solar zenith angle for all vegetation types. There is considerably more scatter evident for albedo than for reflectance.

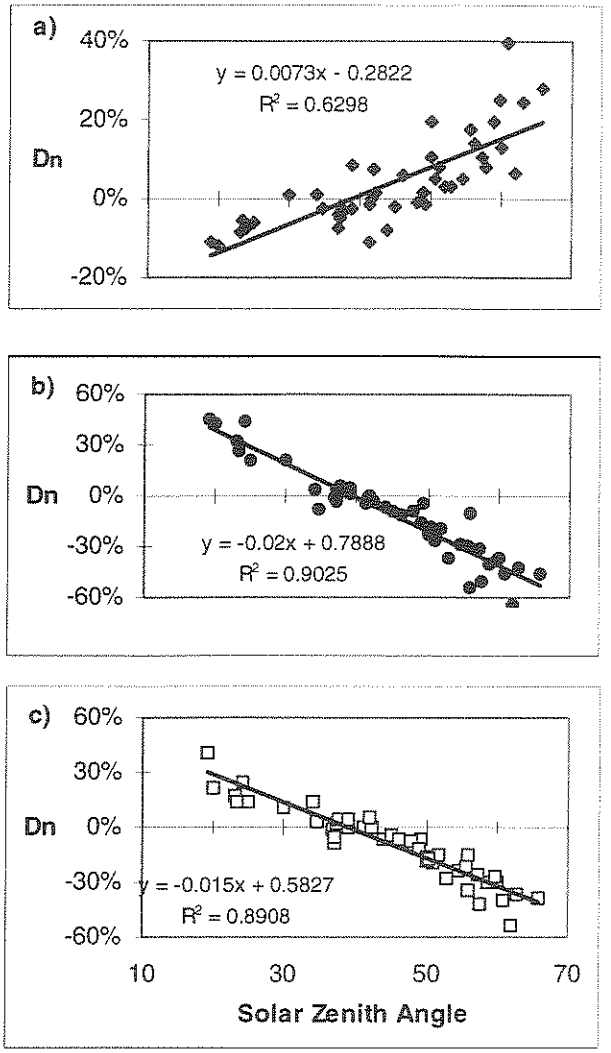

Figure 4. Percentage deviation from reflectance value at Z = 40° for (a) albedo, (b) BR in the red band, and (c) BR in the infrared band. The data is for all vegetation types.

DISCUSSION

The relationship of reflectance to zenith angle appears to hold for all of the surfaces studied. From figure 4 it is evident that solar zenith angle corrections should be made to reflectance data before conversion to albedo.

The hysteresis about noon for the albedo / zenith angle relationship, appears to be an artifact of a physiological response of the vegetation. In order to examine differences in morning and afternoon reflectance values, a number of individual measurements were examined.

Figure 5 shows the distribution of BR in the principal solar plane at a number of solar zenith angles. At the higher zenith angle of 60°, specular reflectance occurs as evidenced by high BR values at large view angles. The effect is more pronounced for infrared wavelengths. Nadir viewed BR does not measure this specular reflection and as a consequence is much lower than the hemispherically integrated value.

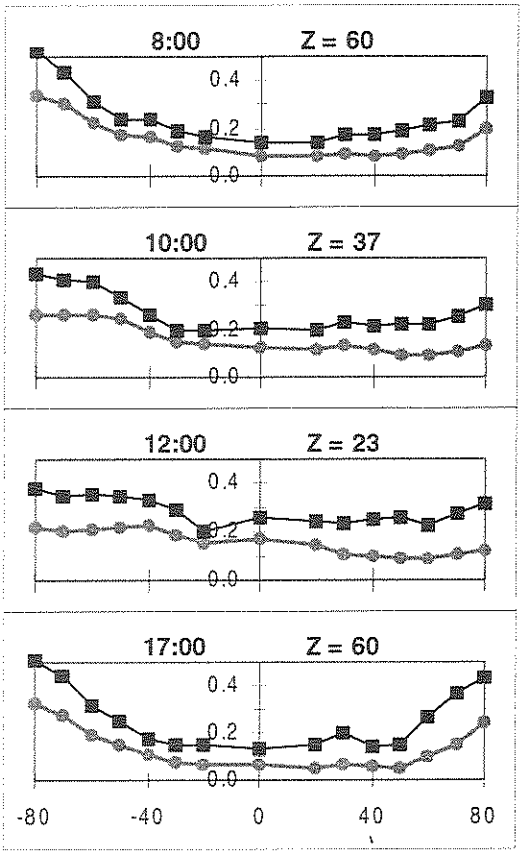

Figure 5. Measured bidirectional distribution in the principal solar plane for both red (circles) and near infrared (squares) over wet heath on a clear summer day.

At the medium solar zenith angles of 40°, specular reflection becomes decreasingly important and the shape of the BR in the principle solar plane becomes less bowl shaped. However the hot-spot effect in the back-scatter direction can be seen to develop at these solar zenith angles. The hot-spot is located at a view zenith angle that approximates the solar zenith and the nadir viewed BR does not incorporate this reflected radiation.

At very low solar zenith angles specular reflection does not occur and the hot spot is within the field of view of the radiometer. As a result the nadir viewed BR approximates the hemispherically integrated reflectance.

The infrared channel exhibits both a more pronounced hot spot effect and greater specular reflectance. The increased importance of specular reflection can also be seen normal to the principal solar plane. The afternoon BR distribution shows greater specular effects at large view angles towards the sun than similar morning solar zenith angles.

The variance of a single 50m transect is examined for a zenith angles of 37° and 62°. Figure 6 shows a frequency histogram of the distribution of individual reflectance measurements for both solar zenith angles in each band.

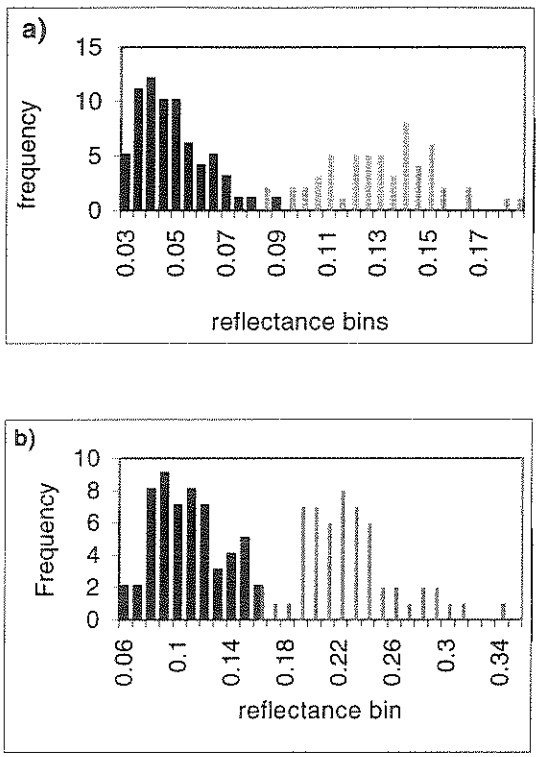

Figure 6. Frequency histogram of the number of pixels at Z = 62° (black bars) and Z = 37° (gray bars) in each reflectance bin for (a) the red band and (b) the near infrared band.

The figure shows that at Z = 37° the absolute values of reflectance is much greater and a greater range of values is shown. There is very little overlap in the ranges of the values for each zenith angle. This occurs for both the red and infrared bands.

It is likely that at large solar zenith angles reflectance is dominated by shadow effects, with fully shaded or fully unshaded values contributing to the range. As the overall incoming radiance is lower the difference between fully illuminated and fully shaded areas may be lower. Increased specular reflection not picked up by the nadir viewing radiometer would contribute to the lower overall reflection.

At small solar zenith angles differences in canopy structure contribute to the signal and shadow effects are confined to smaller portions of a pixel giving a wider range of values, from fully shaded to complete illumination. The incorporation of the hot spot effect and reduced specular effects would contribute to the increased mean reflectance.

From the results of the field measurements it appears that changes in illumination angle due to solar zenith effect both nadir BR and albedo. Expected reflectance at solar zenith angles other than that of the satellite image can be more confidently modelled than expected albedo. Therefore in order to compare satellite images taken at different solar zenith angles, corrections should be applied to reflectance data. The same correction is applicable for all of the low vegetation types studied.

Russell *et al.* [1997] developed a relationship to convert reflectance at a solar zenith angle of 40° to albedo. This relationship could be used to convert solar zenith angle corrected reflectance to an instantaneous albedo value for incorporation into a daily net solar radiation model based on daylength and satellite based estimates of the proportion of cloud cover. Further work will examine the same relationships for forested vegetation types.

CONCLUSION

Short term inter annual changes in the biomass of various vegetation types can be expected as a result of responses to climatic conditions. Daily values of net solar radiation could be calculated from albedo mapped from satellite. For fine resolution mapping of the surface radiation exchange, corrections that can be applied to satellite images taken at different solar zenith angles are required.

The relationship between albedo and zenith angle shows considerable scatter and a hysteresis about noon, possibly due to increased specular reflection, has been found in single day relationships. A more consistent relationship with zenith angle has been found for nadir reflectance in both the red and near infrared bands.

The data presented suggests that separate vegetation specific geometric corrections are not required for the low vegetation types studied. The separation of non-forested vegetation from forest vegetation allows the use of less specific classification systems in image processing.

REFERENCES

Jackson W. D., *The vegetation of Tasmania.* Botany Department, University of Tasmania, Hobart, 1981.

Jarman S. J., G. Kantvilas and M.J. Brown, *Buttongrass moorland in Tasmania. Research Report 2*, Tasmanian Forest Research Council Inc., Hobart, 1988.

Henderson-Sellers, A., Albedo changes: surface surveillance from satellites. *Clim. Change 2*, 275-281, 1980.

Kimes, D. S., and P. J. Sellers, Inferring hemispherical reflectance of the Earth's surface for global energy budgets from remotely sensed nadir or directional radiance values, *Remote Sens. Environ. 18,* 205-223, 1985.

Kirkpatrick J. B., *The disappearing heath.* Tasmanian Conservation Trust Inc., Hobart, 1977.

Kirkpatrick, J. B., and K. J. M. Dickinson, Tasmania Vegetation Map 1:500000, Forestry Commission of Tasmania, Hobart, 1984.

Nunez, N., and J. D. Kalma, Satellite mapping of the surface radiation budget, in *Advances in Bioclimatology 4*, edited by G. Stanhill, pp. 63-124, Springer-Verlag, Berlin, 1996.

Nunez, N., and J.B Kirkpatrick, Rainfall estimation in South-west Tasmania using satellite images and phytosociological calibration. *Int. J. Rem. Sens. 17*, 1583-1600, 1996.

Qi, J., A. R. Huete, F. Cabot, and A. Chehbouni, Bidirectional properties and utilisations of high-resolution spectra from a semi-arid watershed, *Water Resour. Res., 30*, 1271-1279, 1994.

Russell, M. J., N. Nunez, M. A. Chladil, J. A. Valiente, and E. Lopez-Baeza, Conversion of nadir, narrowband reflectance in red and near-infrared channels to hemispherical surface albedo, *Remote Sens. Env. 61*, 16-23, 1997.